
Comparative EIS study of titanium-based materials in high corrosive environments

Pedro P. Socorro Perdomo

Department of Mechanical Engineering,
University of Las Palmas de Gran Canaria, Spain
Email: pedro-socorro@ulpgc.es

Néstor R. Florido Suárez*

Department of Processing Engineering,
University of Las Palmas de Gran Canaria, Spain
Email: nector.florido@ulpgc.es
*Corresponding author

Amparo Verdú-Vázquez

Department of Building Technology,
Universidad Politécnica de Madrid, Spain
Email: amparo.verdu@upm.es

Julia C. Mirza Rosca

Department of Mechanical Engineering,
University of Las Palmas de Gran Canaria, Spain
Email: julia.mirza@ulpgc.es

Abstract: Electrochemical impedance spectroscopy (EIS) is a technique relatively complex and modern that owes its existence to the emergence of electronic circuits. In this work, the behaviour in HCl 20% of three materials, Ti, Ti-15 Mo and Ti-15Mo-5Al fabricated by laser beam melting, was analysed using EIS. Impedance spectra have been obtained at various potentials, from open circuit potential to +2.0 V vs. Ref. Once the profiles of the impedance spectra were analysed, the experimental data were adjusted to an equivalent electrical model. Two models of equivalent circuits were presented: at E_{corr} simple circuit is used while in the passive potential range an equivalent circuit with 2-time constants was used for fit the experimental data. It was concluded that titanium and studied titanium alloys undergo spontaneous passivation due to the oxide film formed on their surface in the reducing acid solution.

Keywords: titanium; titanium alloys; equivalent circuit; electrochemical impedance spectroscopy; EIS; HCl; corrosion.

Reference to this paper should be made as follows: Socorro Perdomo, P.P., Florido Suárez, N.R., Verdú-Vázquez, A. and Mirza Rosca, J.C. (2021) 'Comparative EIS study of titanium-based materials in high corrosive environments', *Int. J. Surface Science and Engineering*, Vol. 15, No. 2, pp.152–164.

Biographical notes: Pedro P. Socorro Perdomo received his first degree in Mechanical Engineering from the University of León, Spain. He is an Assistant Professor at the University of Las Palmas de Gran Canaria, Spain. He is a member of Nanomaterials and Corrosion Research group (NanCorr). He is working in the Department of Mechanical Engineering. His scientific interests mainly cover the field of industrial materials, biomaterials and nanomaterials.

Néstor R. Florido Suárez received his first degree in Industrial Engineering from the University of Las Palmas de Gran Canaria, Spain. He is a part-time Lecturer at the University of Las Palmas de Gran Canaria, Spain. He is a member of Nanomaterials and Corrosion Research group (NanCorr). He is working in the Department of Process Engineering. His scientific interests mainly cover the field of biomedicine, biotechnology, industrial materials, and nanomaterials.

Amparo Verdú-Vázquez is an Associate Professor at the Polytechnic University of Madrid. She is working in the Department of Building Technology at the Higher Technical School of Building. Her scientific interests mainly cover technology transfer projects. She has devoted her time to research in materials and their applications in industry and education.

Julia C. Mirza Rosca is a Professor at the University of Las Palmas de Gran Canaria, Spain. She is working in the Department of Mechanical Engineering. She is the Head of Nanomaterials and Corrosion Research group (NanCorr). Her scientific interests mainly cover the field of electrochemical processes, corrosion, biomaterials and nanomaterials.

1 Introduction

Titanium has a great resistance to corrosion (Peters and Leyens, 2003) and this explains the great influence that titanium is acquiring in the chemical, biomedical and power generation industries. The price of titanium is high but due to the intrinsic nature of these industries, it is profitable because it lowers the maintenance costs.

Titanium is normally used in those areas where stainless steel does not provide sufficient resistance to corrosion; titanium and titanium alloys have high tensile strength, high strength-to-weight ratio and excellent corrosion resistance due to a native oxide film formed on the surface. Therefore, it is found in facilities exposed to strong inorganic acids but unfortunately, this protective passive film is susceptible to failure in HCl environment industries. In these industries, less mechanical resistance is required than in others, but greater resistance to corrosion, which is why titanium and titanium alloys are used. Their uses are many, among which are: condensers, heat exchangers, turbines, purifiers, storage tanks, pipes, pumps, valves, etc.

Pure titanium undergoes an allotropic phase transformation at 882°C, changing from a body-centred cubic crystalline structure (phase α) above the transformation temperature, to a compact hexagonal structure (phase β) below this temperature (Vasylyev et al., 2020). The exact temperature at which the transformation takes place strongly depends on the interstitial and substitutional elements found in this metal. It depends, ultimately, on the purity of the material.

The existence of two different crystalline structures makes possible to carry out thermal treatments with total transformation, since allotropic forms present a different behaviour against deformation: the phase α , little deformable and resistant to room temperature and the phase β , easily deformable (Kaur and Singh, 2019).

The alloy elements that change the allotropic transformation temperature can be divided into three groups, α -stabilisers (Al, O, N, C), β -stabilisers (V, Mo, Nb, Ta, Fe, Mn, Cr, Ni, Cu, Si) and neutralisers (Zr, Sn).

It is common to divide titanium alloys into three groups, depending on the phases present: alloys α and almost- α ; alloys α - β and alloys β . The titanium β alloys have a higher content of β phase stabilising elements and a lower content of α phase stabilisers than the alloys α - β . They are characterised by their high hardening capacity, since, for example, in small thicknesses they reach air hardening and completely retain the β phase (Kolli and Devaraj, 2018). They are titanium alloys with better aptitude for conformation by plastic deformation, being able to deform in cold much better than the α or α - β alloys (Noori Banu and Devaki Rani, 2019).

Ti-Mo alloys are shown as one of the large families of alloys within β -Ti alloys. Molybdenum is a β phase stabilising element, so it decreases the transition temperature from β structure to α structure and stabilises the β phase. This temperature is directly increased by the presence of β phase stabilising alloy elements and in many cases, this temperature is below room temperature, so alloys with this characteristic have β structure in use at room temperature.

There are many studies regarding the properties of titanium alloys with different concentrations of molybdenum starting at 3% Mo till 20% Mo, generally for biomedical applications. These alloys were most of them obtained by arc melting in an ultra-pure argon atmosphere (Oliveira and Guastaldi, 2008, 2009; Oliveira et al., 2007, 2009; Ho et al., 1999; Cardoso et al., 2014), but some of them were synthesised by laser-assisted (Almeida et al., 2012), using a DC magnetron sputtering method (Habazaki et al., 2003) or direct energy deposition – laser additive manufacturing (Bhardwaj et al., 2019).

There are many techniques used in additive manufacturing, depending on the process used or the types of materials are needed to use. On some occasions, for example in the industrial environment, it is necessary to manufacture metal parts, and it is then when such innovative techniques as fusion or sintering of metal powder by electron beam namely electron beam melting come into play. This is a technology that makes possible to build geometrically complex parts and is very similar to selective laser sintering, but in which the energy source is more powerful.

In this work, the behaviour in HCl 20% of three materials, Ti, Ti-15 Mo and Ti-15Mo-5Al fabricated by laser beam melting, was analysed using electrochemical impedance spectroscopy (EIS).

2 Experimental

Titanium and the following titanium alloys were studied: Ti-15Mo and Ti-15Mo-5Al (the numbers signify the wt. %) with the composition given in Table 1 and obtained by Electron Beam Melting (Arcam AB, Sweden) from high purity metallic gas atomised powders. The samples were built layer-by-layer on a titanium commercially pure grade 2 as substrate and selectively melted at a voltage of 60 kV and electron beam size of

200 μm . Due to the high reactivity of titanium, the process was carried out in a controlled atmosphere under high purity argon gas. The samples obtained are in the form of flat discs (approx. 0.5 cm in diameter) and the impedance tests have been carried out in a 20% HCl solution. The samples were initially polished on a Struers Tegrapol-11 polishing machine with emery discs of various sizes (800 to 2,500) and then with diamond paste (0.1 μm) on a polishing cloth. The surface of each sample has been left as a mirror surface to ensure reproducibility of results. Subsequently, the polished samples have been washed with acetone and then in an ultrasonic cleaner for ten minutes. Finally, they have been rinsed with bi-distilled water and air dried at room temperature.

The electrochemical tests have been done at 25°C using a cell containing 100 ml of electrolyte. The flat surface of each sample was brought into contact with the solution by means of a hanging meniscus assembly. To measure the potential of the analysed samples at all times, a saturated calomel reference electrode (SCE) was used; a cylindrical, high-surface platinum mesh was used as a counter electrode.

Impedance spectra have been obtained at various potentials, from open circuit potential to +2.0 V and therefore a set of potentiostat and blocking amplifier PARC 263 A and PARC 5210 respectively have been used. At each potential, single sine wave recordings were made at frequencies between 100 mHz and 100 kHz.

3 Results and discussion

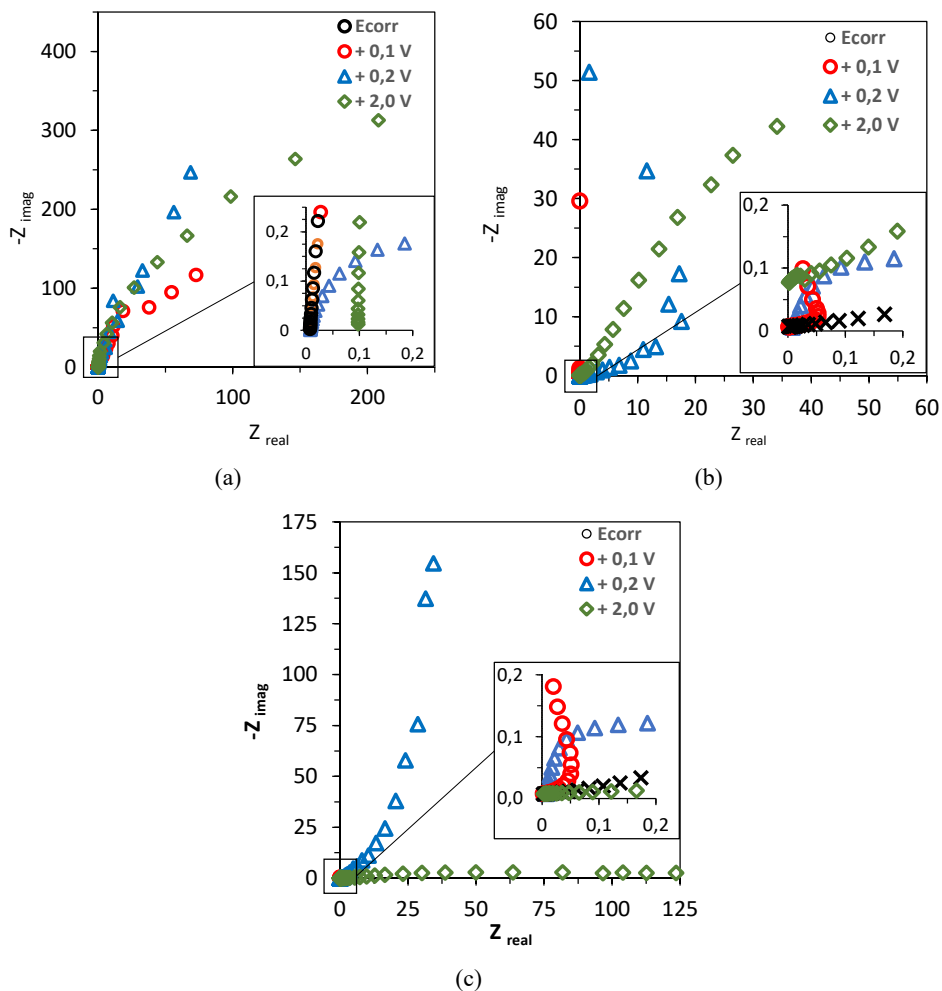
EIS is a technique relatively complex and modern that owes its existence to the emergence of electronic circuits fast enough and sensible enough to create and evaluate a variable frequency and phase signal (Ciucci, 2019; Gabrielli, 2020; Mareci et al., 2007; Niaz, 2020). It is a non-destructive technique (in case of tests in equilibrium conditions), particularly sensible to small modifications in the system, which permits the characterisation of the properties of the materials and the mechanism of electrochemical processes (Goulart et al., 2007; Oliveira and Guastaldi, 2009; Mareci et al., 2010). For many materials and electrochemical processes, the impedance varies with the frequency and the applied potential and therefore we relate it to the properties of these materials. This is due to the physical characteristics of the material, to the electrochemical processes that take place on the surface or a combination of both. Therefore, if we carry out impedance measurements in a suitable range of frequencies, the spectra obtained relate the physical and chemical properties of the samples to the mechanism of the electrochemical process that takes place.

The interpretation of the impedance spectrum requires the selection of an appropriate electrical system that fits the experimental data (González and Mirza-Rosca, 1999). Through the model, the obtained measurements using this technique provide information related to the dissolution resistance, polarisation resistance and double-layer capacitance of Helmholtz. The dissolution resistance is obtained at high frequencies and the data acquired at low frequencies give information on the kinetics of the reaction. According to the model that is proposed and the way to propose it, information of the characteristic parameters of the process can be obtained.

Firstly, the obtained results for the studied alloys at various applied passivation potentials will be commented analysing the most significant graphs (Nyquist and Bode graphs).

As can be seen in the Nyquist diagrams (see Figure 1), at the corrosion potential the radius of the semicircle is very small, which indicates a low polarisation resistance or what is the same, a low resistance to corrosion because on the material begins to form a passive layer. As the potential increases, the resistance to polarisation and implicitly the resistance to corrosion increases.

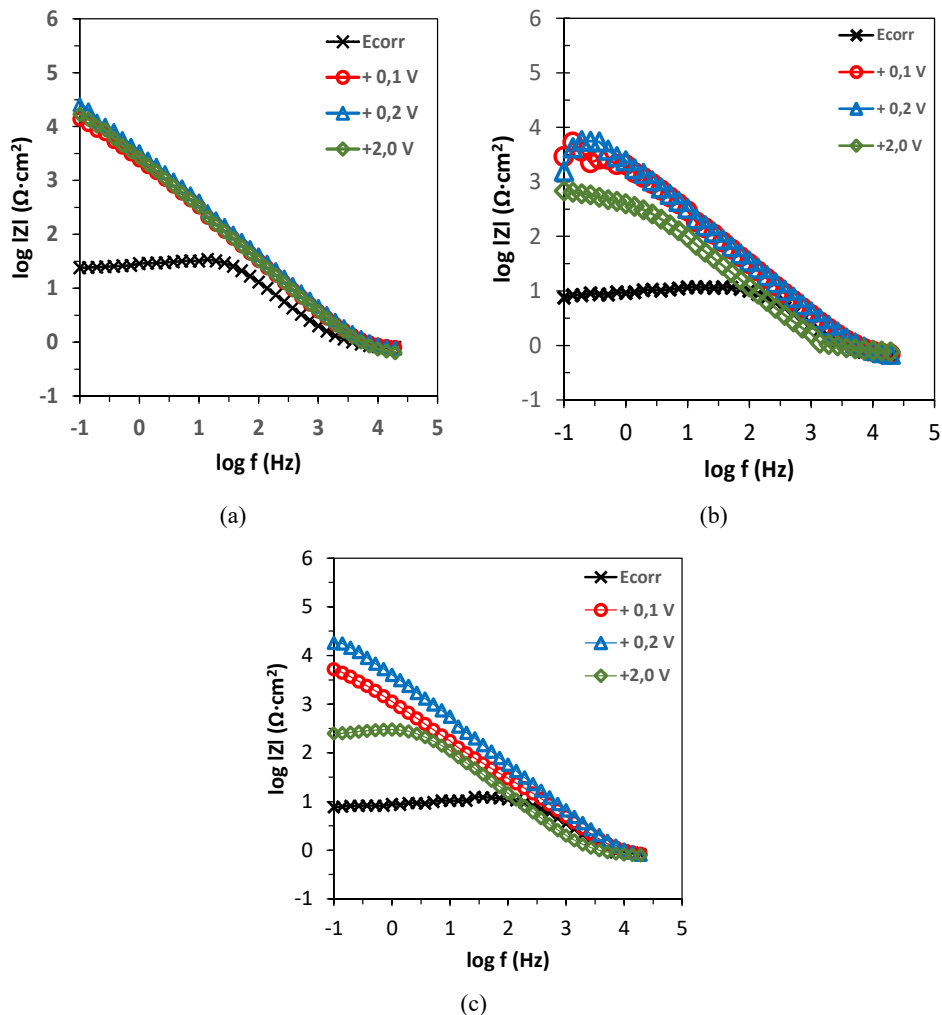
Figure 1 Nyquist plots at E_{corr} , 0.1V vs. SCE, 0.2V vs. SCE and 2.0V vs. SCE for (a) Ti, (b) Ti-15Mo and (c) Ti-15Mo-5Al (see online version for colours)



It can be observed the beginning of another semicircle at 100 mV which translates into the beginning of a new stage of the process of passivation. At 200 mV the passive layer increases in thickness and the resistance to corrosion is also greatly increased. As potential increases the materials are still very stable in HCl 20% and the radius of the semi-circle in the Nyquist diagram undergoes a considerable increase which translates into an increase of the polarisation resistance (R_p) or, in other words, an increase of the resistance to corrosion.

In the Bode-IZI diagrams (see Figure 2) a strong displacement of the impedance module towards higher values is observed, clearly indicating an increase in corrosion resistance due to the formation of the passive layer on the surface of the three materials.

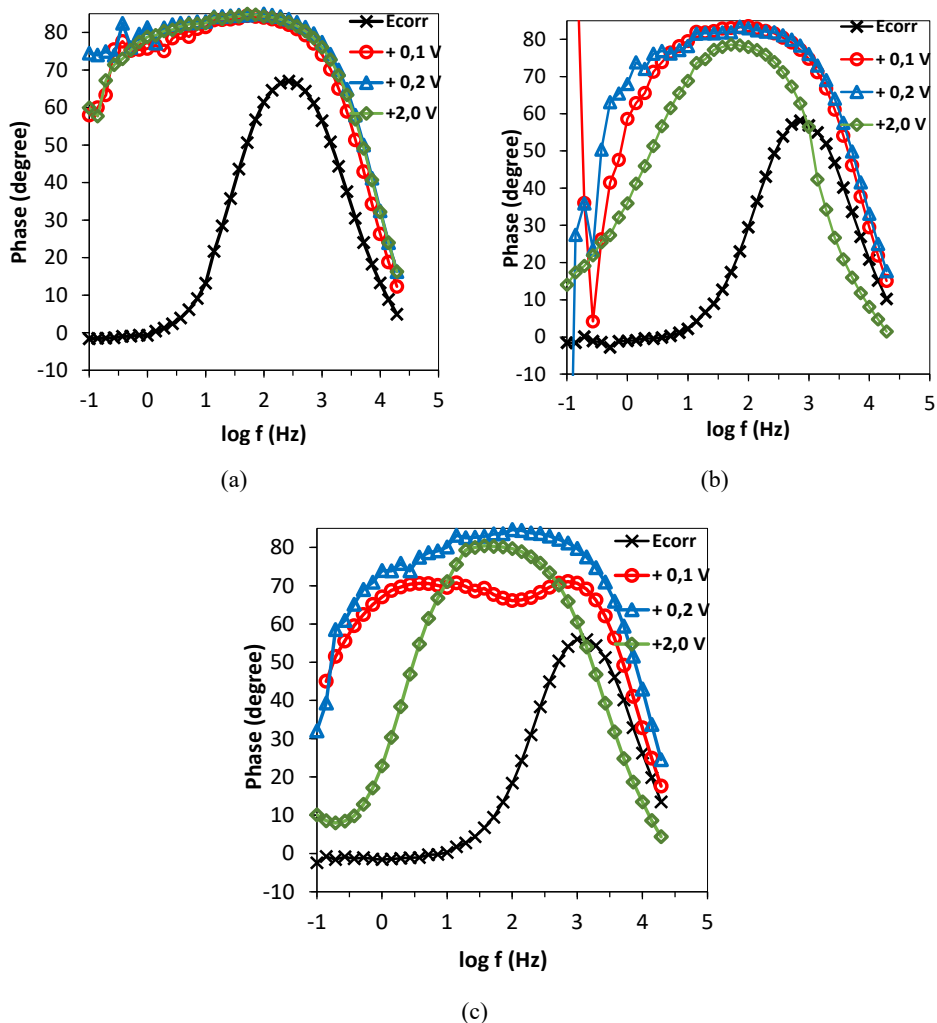
Figure 2 Bode-IZI plots at E_{corr} , 0.1V vs. SCE, 0.2V vs. SCE and 2.0V vs. SCE for (a) Ti, (b) Ti-15Mo and (c) Ti-15Mo-5Al (see online version for colours)



The profile of the results at 200 mV is very similar and a little higher than that obtained at 100 mV due to the increase in thickness of the passive layer with the increase in potential. The slopes of the graphs follow -1 at both 100 mV and 200 mV (including till 2 V) indicating the capacitive behaviour of the passive film formed.

In the Bode-phase diagrams (see Figure 3), a typical behaviour of the initial nucleation of a passive layer on the surface of the metal is observed in the corrosion potential.

Figure 3 Bode – phase plots at E_{corr} , 0.1V vs. SCE, 0.2V vs SCE and 2.0V vs SCE for (a) Ti, (b) Ti-15Mo and (c) Ti-15Mo-5Al (see online version for colours)



As the potential increases, the formed film increases in thickness and has a capacitive response illustrated by a phase angle close to 90° over a wide range of frequencies. This phenomenon is associated with an increase in the capacity (C), which is related to an increase in effective surface area.

Once the profiles of the impedance spectra are analysed, the obtained experimental data will be adjusted to an equivalent electrical model. An equivalent circuit is a combination of passive elements (resistances, capacitances, inductors and other forms of distributed impedance) that give a corrosion-like response in the frequency range under analysis.

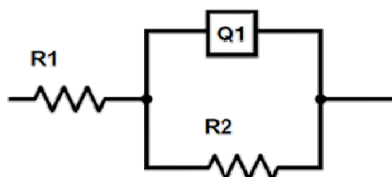
When the EIS experimental data is analysed, it is compared with the response of an equivalent electrical circuit and the values of the different electrical parameters are

measured. In the case of corrosion processes, these values are used to obtain information on both the corrosion resistance of the material and the corrosion mechanism.

In the use of equivalent electrical circuits for EIS data analysis it is necessary to consider that there are, normally, a wide variety of circuit configurations that can reproduce, with high accuracy, the same response that is obtained experimentally from a real process.

The equivalent circuit represented in Figure 4 corresponds to the simplest one with is possible to adjust the experimental data, when only the load transfer is taking into account. This circuit has been used to fit the experimental data obtained at the corrosion potential. In this case, the theoretical transfer function, $Z(\omega)$, is represented by a parallel combination of a resistor R2 and a capacitance Q1, both in series with another resistor R1.

Figure 4 Equivalent circuit used for fit the experimental data at E_{corr}



R1 represents the resistance of the electrolyte, whose value can be calculated by a sweep at high frequencies. R2 is the term for load transfer resistance, R_{ct} .

The capacity of the double layer Cdl (Q1) is related to the interactions that have place at the electrode/electrolyte interface.

A constant phase element (CPE) has been chosen instead of an ideal capacitance (Ibriş and Mirza Rosca, 2002) in order to be able to take into account the heterogeneities of the passivated surface.

The impedance of a CPE is given by Boukamp (1986):

$$Q = Z_{CPE}(\omega) = [C(j\omega)^n]^{-1}$$

For this reason, one of the parameters obtained when modelling the system is the coefficient of ideality 'n', so that the response of the real system is closer to the ideal as the value of n is closer to the unit and therefore the surface is more homogeneous. So, for $n = 1$, the CPE element reduces to a capacitor with a capacitance Y_0 and for $n = 0$ to a simple resistance.

The experimental data at corrosion potential fit the equation 4 and the fitting results are presented in Table 1.

R2 represents the polarisation resistance at the interface metal/passive film so, represents the corrosion resistance of the metal. It can be observed that this resistance increases with the addition of the Mo which is well-known that improves the pitting and crevice corrosion resistance enhancing the passive film resistance by decreasing the number of defects points in the film. R2 increases even more when Al is added due to the formation of a compact and protective Al_2O_3 film.

Table 1 Values of the fitted parameters of the experimental data with the equivalent circuit with one-time constant

<i>Alloy</i>	R_1 (Ωcm^2)	Y_0 (Fcm^{-2})	N	R_2 (Ωcm^2)
Ti	0.81	8.9×10^{-4}	0.62	14.7
Ti-15Mo	0.64	8.2×10^{-4}	0.64	16.9
Ti-15Mo-5Al	0.83	7.9×10^{-4}	0.70	17.2

For potentials higher than the corrosion potential, the single circuit has unacceptable setting errors and therefore a circuit with two time constants which takes into account the structure of the passive layer already formed on the surface of the materials has been used. It should be recalled that in this study the main objective is to check the validity of the EIS technique for this type of system, so it is not so important the selected equivalent circuit, but that it allows to reveal the existence or not of differences in the electrochemical behaviour of the material depending on the applied passivation potential or the composition of the employed material.

The circuit that best fits the experimental data in these cases is the one presented in Figure 5.

The component elements are:

R_1 dissolution resistance

Q_1 CPE of the porous external passive layer

R_2 resistance of the external porous layer

Q_2 CPE of the inner passive layer

R_3 polarisation resistance.

First, we calculate the admittance of the parallel combination (R_2Q_1):

$$\frac{1}{Z_{eq}} = \frac{1}{Z_{R_2}} + \frac{1}{Z_{Q_1}} \quad (1)$$

Even a CPE was used for experimental data fitting, the obtained value is taken as the capacitance in the forthcoming discussion:

$$\frac{1}{Z_{eq}} = \frac{1}{Z_{R_2}} + j \omega C_1 \quad (2)$$

And after multiplying by R_2 :

$$Z_{eq} = \frac{R_2 - j(\omega C_1 R_2^2)}{1 + (\omega C_1 R_2^2)} \quad (3)$$

We added the ohmic resistance of the electrolyte:

$$Z_{eq} = R_1 \frac{R_2 - j(\omega C_1 R_2^2)}{1 + (\omega C_1 R_2^2)} \quad (4)$$

The total impedance is,

$$Z_{eq} = R_1 + \frac{1}{j\omega C_1 + \frac{1}{R_2 + \frac{1}{R_3 + j\omega C_2}}} \quad (5)$$

After standard calculations, the following equation was obtained:

$$Z_{eq} = R_1 + \frac{A - w^2 AB + w^2 CD}{(1 - w^2 B)^2 + w^2 C^2} + j\omega \frac{D - AC - w^2 BD}{(1 - w^2 B)^2 + w^2 C^2} \quad (6)$$

where

$$A = R_1 + R_2$$

$$B = \tau_1 \tau_2$$

$$C = \tau_1 + \tau_2 + C_1 R_3$$

$$D = \tau_2 R_2$$

$\tau_1 \equiv$ time constant of porous film [s]

$\tau_2 \equiv$ time constant of compact film [s]

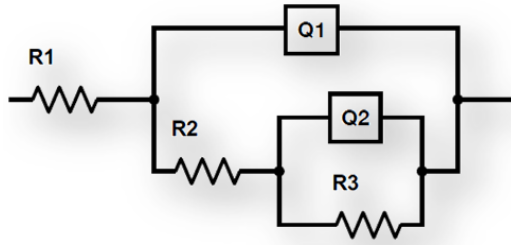
The first coupled parameters R_2 and Q_1 describe the processes at the outer porous passive film/solution interface and the second coupled parameters R_3 and Q_2 represent the properties of the reactions at the inner barrier layer/metal interface. The results of the fitting are presented in Table 2 and in Figure 6 residual error plots are shown for fits using the first (see Figure 4) and the second equivalent circuit (see Figure 5). From the value of the chi-square and the distribution of errors versus frequency, it can be seen that when a model with two time constants is employed, the quality of the fit is improved, so this circuit had to be considered.

Table 2 Parameters obtained from fitting EIS data for Ti and Ti alloys at different potentials

Alloy	Pot.vs OCP	R_1 (Ωcm^2)	Y_0 (Fcm^{-2})	n	R_2 (Ωcm^2)	Y_0 (Fcm^{-2})	n	R_3 ($\text{k}\Omega\text{cm}^2$)
Ti	0.1	0.79	1.8×10^{-4}	0.82	660.2	6.2×10^{-3}	0.95	7.3
	0.2	0.77	1.6×10^{-4}	0.84	680.3	5.3×10^{-3}	0.96	8.2
	2.0	0.64	2.0×10^{-4}	0.87	522.4	6.8×10^{-3}	0.90	7.1
Ti-15Mo	0.1	0.69	2.1×10^{-4}	0.80	720.8	5.5×10^{-3}	0.96	9.6
	0.2	0.70	1.9×10^{-4}	0.82	786.4	5.2×10^{-3}	0.93	10.1
	2.0	0.77	2.3×10^{-4}	0.85	702.3	5.9×10^{-3}	0.89	9.2
Ti-15Mo-5Al	0.1	0.84	2.3×10^{-4}	0.79	782.8	5.2×10^{-3}	0.91	11.7
	0.2	0.81	2.0×10^{-4}	0.82	880.5	4.8×10^{-3}	0.94	12.2
	2.0	0.79	2.3×10^{-4}	0.88	723.4	5.2×10^{-3}	0.88	10.6

The parameter R_1 has a value from 0.64 to 0.84 Ωcm^2 and is ascribed to electrolyte resistance and during the experiments there is no appreciable variation of the values which mean that no ions released in the solution during the passive potential range.

Figure 5 Equivalent circuit used for fit the experimental data at passivation potentials



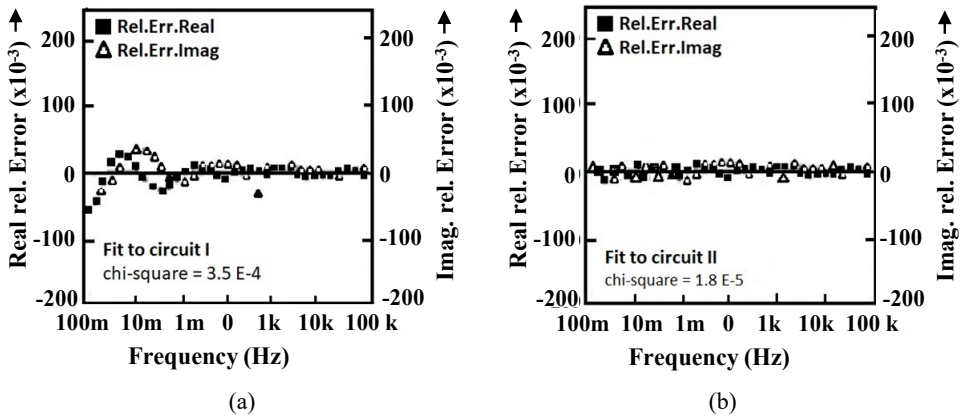
The values of R_2 are lower than R_3 values, reflecting that the outer porous film exhibits lower resistance than the inner barrier layer. High values of R_3 are observed at all potential and an increase with Mo concentration and Al addition, confirming the formation of a passive layer with high corrosion protection ability.

It can be observed that the fitted values of R_3 increase with potential while Y_0 decreases, indicating that the thickness and stability of the protective oxide film increased in passivation potential range.

The residual error plots using equivalent circuits with one and two-time constant are shown in Figures 6(a) and 6(b).

It can be observed that with the second equivalent circuit the fitting quality is very good ($\text{chi-square} = 1.8 \cdot 10^{-5}$) better that with simple circuit.

Figure 6 Residual error plots for fits using (a) one and (b) two time constant



4 Conclusions

- 1 Titanium and titanium alloys undergo spontaneous passivation due to the oxide film formed on their surface in the reducing acid solution.
- 2 The passive potential range is very large for the studied materials in HCl 20% (exceeding 2.0 V).
- 3 As the potential increases, the thickness of the passive film increases and it has a capacitive response (good stability) over a wide frequencies range.

- 4 Two models of equivalent circuits describing the spontaneous passivation of Ti, Ti-15Mo and Ti-15Mo-5Al in HCl 20% were presented. At E_{corr} simple Randles circuit is used while in the passive potential range an equivalent circuit with 2 time constants was used for fit the experimental data. Also a CPE was employed instead of the capacitive element.
- 5 For all the analysed materials there are no released ions in the solution during the passive potential range.
- 6 The addition of Mo and Al generates the formation of a passive layer with higher corrosion protection ability than for titanium.
- 7 In a HCl 20% solution, the oxide film on Ti and Ti studied alloys fabricated by laser beam melting exhibits a high corrosion resistance and a long-term stability, which recommends their use for the manufacture of metallic parts employed in aggressive industrial environments.

References

- Almeida, A. et al. (2012) 'Laser-assisted synthesis of Ti-Mo alloys for biomedical applications', *Materials Science and Engineering C*, Vol. 32, No. 5, pp.1190–1195, DOI: 10.1016/j.msec.2012.03.007.
- Bhardwaj, T. et al. (2019) 'Direct energy deposition – laser additive manufacturing of titanium-molybdenum alloy: parametric studies, microstructure and mechanical properties', *Journal of Alloys and Compounds*, Vol. 787, pp.1238–1248, DOI: 10.1016/j.jallcom.2019.02.121.
- Boukamp, B.A. (1986) 'A nonlinear least squares fit procedure for analysis of' imittance data of electrochemical systems', *Solid State Ionics*, Vol. 20, pp.31–44, DOI: 10.1015/0167-2738(86)90031-7.
- Cardoso, F.F. et al. (2014) 'Ti-Mo alloys employed as biomaterials: Effects of composition and aging heat treatment on microstructure and mechanical behavior', *Journal of the Mechanical Behavior of Biomedical Materials*, Vol. 32, pp.31–38, DOI: 10.1016/j.jmbbm.2013.11.021.
- Ciucci, F. (2019) 'Modeling electrochemical impedance spectroscopy', *Current Opinion in Electrochemistry*, DOI: 10.1016/j.coelec.2018.12.003.
- Gabrielli, C. (2020) 'Once upon a time there was EIS', *Electrochimica Acta*, Vol. 331, pp.1–20 DOI: 10.1016/j.electacta.2019.135324.
- González, J.E.G. and Mirza-Rosca, J.C. (1999) 'Study of the corrosion behavior of titanium and some of its alloys for biomedical and dental implant applications', *Journal of Electroanalytical Chemistry*, Vol. 471, No. 2, pp.109–115, DOI: 10.1016/S0022-0728(99)00260-0.
- Goulart, P.R. et al. (2007) 'Dendritic microstructure affecting mechanical properties and corrosion resistance of an Al-9 wt% Si alloy', *Materials and Manufacturing Processes*, Vol. 22, No. 3, pp.328–332, DOI: 10.1080/10426910701190345.
- Habazaki, H. et al. (2003) 'Formation of barrier-type amorphous anodic films on Ti-Mo alloys', *Surface and Coatings Technology*, Vols. 169–170, pp.151–154, DOI: 10.1016/S0257-8972(03)00216-0.
- Ho, W.F., Ju, C.P. and Chern Lin, J.H. (1999) 'Structure and properties of cast binary Ti-Mo alloys', *Biomaterials*, Vol. 20, No. 22, pp.2115–2122, DOI: 10.1016/S0142-9612(99)00114-3.
- Ibrış, N. and Mirza Rosca, J.C. (2002) 'EIS study of Ti and its alloys in biological media', *Journal of Electroanalytical Chemistry*, Vol. 526, Nos. 1–2, DOI: 10.1016/S0022-0728(02)00814-8.

- Kaur, M. and Singh, K. (2019) 'Review on titanium and titanium based alloys as biomaterials for orthopaedic applications', *Materials Science and Engineering C*, February, Vol. 102, pp.844–862, DOI: 10.1016/j.msec.2019.04.064.
- Kolli, R.P. and Devaraj, A. (2018) 'A review of metastable beta titanium alloys', *Metals*, Vol. 8, No. 7, pp.1–41, DOI: 10.3390/met8070506.
- Mareci, D. et al. (2010) 'The corrosion of dental amalgam in some commercial mouthwash solutions', *Revista de Chimie*, Vol. 61, No. 5, pp.443–448.
- Mareci, D., Ungureanu, G., Aelenci, N., Chelariu, R. and Rosca, J.C.M. (2007) 'EIS diagnosis of some dental alloys in artificial saliva', *Environmental Engineering and Management Journal* Vol. 6, No. 4, pp.313–317.
- Niaz, A. (2020) 'Corrosion and passive film study of cermet-coatings deposited by high-velocity oxygen fuel method in an acidic environment', *International Journal of Surface Science and Engineering*, DOI: 10.1504/IJSURFSE.2020.110533.
- Noori Banu, P.S. and Devaki Rani, S. (2019) 'Microstructure evaluation and modelling the tensile strength and yield strength of titanium alloys', *International Journal of Microstructure and Materials Properties*, DOI: 10.1504/ijmmp.2019.10019610.
- Oliveira, N.T.C. and Guastaldi, A.C. (2008) 'Electrochemical behavior of Ti-Mo alloys applied as biomaterial', *Corrosion Science*, Vol. 50, No. 4, pp.938–945, DOI: 10.1016/j.corsci.2007.09.009.
- Oliveira, N.T.C. and Guastaldi, A.C. (2009) 'Electrochemical stability and corrosion resistance of Ti-Mo alloys for biomedical applications', *Acta Biomaterialia*, Vol. 5, No. 1, pp.399–405, DOI: 10.1016/j.actbio.2008.07.010.
- Oliveira, N.T.C. et al. (2007) 'Development of Ti-Mo alloys for biomedical applications: microstructure and electrochemical characterization', *Materials Science and Engineering A*, Nos. 452–453, pp.727–731, DOI: 10.1016/j.msea.2006.11.061.
- Oliveira, N.T.C. et al. (2009) 'Photo-electrochemical investigation of anodic oxide films on cast Ti-Mo alloys. I. Anodic behaviour and effect of alloy composition', *Electrochimica Acta*, Vol. 54, No. 5, pp.1395–1402, DOI: 10.1016/j.electacta.2008.08.074.
- Peters, M. and Leyens, C. (2003) *Titanium and Titanium Alloys: Fundamentals and Applications*, *Titanium and Titanium Alloys Fundamentals and Applications*, Wiley-VCH Verlag GmbH & Co, Weinheim, Germany, ISBN 3-527-30534-3.
- Vasylyev, M.A., Mordiyuk, B.N., Bevez, V.P., Voloshko, S.M. and Mordiyuk, O.B. (2020) 'Ultrasonically nanostructured electric-spark deposited Ti surface layer on Ti6Al4V alloy: enhanced hardness and corrosion resistance', *International Journal of Surface Science and Engineering*, DOI: 10.1504/IJSURFSE.2020.105874.